

Shot noise spectrum of artificial Single Molecule Magnets: measuring spin-relaxation times via the Dicke effect.

L.D. Contreras-Pulido¹ and R. Aguado¹

¹*Departamento de Teoría de la Materia Condensada,
Instituto de Ciencia de Materiales de Madrid, CSIC, Cantoblanco 28049, Madrid, Spain*

(Dated: July 9, 2009)

We investigate theoretically shot noise in an artificial Single Molecule Magnet based upon a CdTe quantum dot doped with a *single* $S=5/2$ Mn spin and gated in the hole sector. Mn-hole exchange anisotropy is shown to lead to profound consequences on noise, like super-Poissonian behaviour. We report on a novel effect, similar to the Dicke effect in Quantum Optics, that allows to *separately* extract the hole and Mn spin relaxation times using frequency-resolved shot noise measurements. We expect that our findings may have further relevance to experiments in other $S > 1/2$ systems including transport through Mn_{12} molecules and STM spectroscopy of magnetic atoms.

PACS numbers:

Single Molecule Magnets (SMMs) combine properties of a magnet with those of a nanostructure. This makes SMMs a useful platform to merge concepts and applications of spintronics and nanoelectronics [1]. In a transistor setup, SMMs behave as Quantum Dots (QDs). This allows detailed Coulomb Blockade (CB) level spectroscopy of prototypical examples, like Mn_{12} [2, 3] or endofullerene $N@C_{60}$ [4]. The experimental extraction of their intrinsic properties is, however, very challenging because little is known about the precise role of various sample-preparation steps like the attachment of leads. An alternative route is to study artificial counterparts to a SMM, like a CdTe QD doped with a single Mn^{+2} ion with spin $S = 5/2$ (Fig. 1). This proposal is based on recent experiments where these QDs (without contacts) are optically probed [5, 6, 7, 8, 9]. When doped with a single hole, the system behaves as a SMM with magnetization steps and hysteresis [10]. Furthermore, its transport properties depend on the quantum state of the Mn spin, giving rise to remarkable phenomena like hysteretic CB [11].

While dc transport entails considerable information, a complete understanding requires to go beyond and study shot noise [12], which we address here. Our results show that exchange anisotropy leads to super-Poissonian shot noise due to lack of relaxation of the Mn spin. Interestingly, a novel effect at finite frequencies, similar to the Dicke effect in Quantum Optics [13], allows to *separately* measure the hole and Mn spin relaxation times (Fig. 4).

Model.— The minimal model of an artificial SMM reads $H_{eff}^{QD} = \sum_{\sigma} \varepsilon_h d_{\sigma}^{\dagger} d_{\sigma} + H_{eff}^{exch}$. The first term describes confined holes within the QD, the second term describing the effective hole-Mn anisotropic exchange is

$$H_{eff}^{exch} = [J_{\parallel} \tau_h^z M^z + \frac{J_{\perp}}{2} (\tau_h^+ M^- + \tau_h^- M^+)], \quad (1)$$

with $J_{\parallel} = J$ and $J_{\perp} = \alpha J$ ($\alpha \leq 1$). $M^{z,\pm}$ are the Mn spin operators and $\tau_h^{z,\pm}$ are Pauli matrices operating in the hole lowest energy doublet $|\uparrow_h\rangle = a|3/2, +3/2\rangle +$

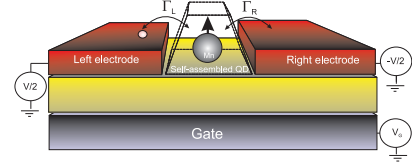


FIG. 1: (Color online) Schematics of the artificial SMM based on a CdTe QD doped with a single Mn^{+2} ion and coupled to metallic reservoirs (tunnelling rates Γ_L and Γ_R and chemical potentials $\mu_{L/R} = \pm V/2$). V_G is the gate voltage.

$b|3/2, -1/2\rangle$ and $|\downarrow_h\rangle = a|3/2, -3/2\rangle + b|3/2, +1/2\rangle$. H_{eff}^{QD} is obtained from the full problem $H = \sum_n \varepsilon_n d_n^{\dagger} d_n + J_h \tilde{S}_h(\vec{r}_M) \vec{M}$ after projecting onto the $|\uparrow_h\rangle, |\downarrow_h\rangle$ subspace [11]. d_n^{\dagger} creates a confined hole in the spin-orbital $\psi_n(\vec{r})$, described by a six band Kohn-Luttinger Hamiltonian, and $\tilde{S}_h(\vec{r}_M)$ is the hole spin density evaluated at the Mn location. $J = J_h |\psi(\vec{r}_M)|^2$, $J_h \simeq 60 \text{ eV} \text{ \AA}^3$ being the hole-Mn exchange coupling constant of CdTe. Due to strong spin-orbit coupling, exchange is highly anisotropic and spin flips are suppressed $\langle \downarrow_h | S_h^- | \uparrow_h \rangle \approx 0$ unless there is some heavy hole-light hole mixing due to asymmetry $b \neq 0$, $\alpha = J_{\perp}/J \neq 0$ [14, 15].

Quantum Master Equation (QME).— The full Hamiltonian including the coupling to reservoirs reads $H = H_{eff}^{QD} + \sum_{\alpha \in L,R} H_{res}^{\alpha} + H_T^{\alpha}$. The Hamiltonian of each hole reservoir is $H_{res}^{\alpha} = \sum_{k_{\alpha}, \sigma} \varepsilon_{k_{\alpha}, \sigma} c_{k_{\alpha}, \sigma}^{\dagger} c_{k_{\alpha}, \sigma}$ whereas $H_T^{\alpha} = \sum_{k_{\alpha}, \sigma} V_{k_{\alpha}} c_{k_{\alpha}, \sigma}^{\dagger} d_{\sigma} + H.c.$ describes tunneling. The QME for the reduced density matrix, $\rho(t)$, is obtained after applying a Born-Markov approximation [11] with respect to $H_T^{L/R}$, $\dot{\rho}(t) = \mathcal{L}\rho(t)$. The dissipative dynamics is governed by a Liouvillian superoperator \mathcal{L} which contains the forward/backwards (\pm) transition rates $\Gamma_{N, N \mp 1}^{\pm} = \sum_{\alpha=L,R} \Gamma_{\alpha} f_{\alpha}^{\pm} (E_N - E_{N \mp 1}) \sum_{\sigma} |\langle N | d_{\sigma}^{\pm} | N \mp 1 \rangle|^2$ between eigenstates of H_{eff}^{QD} . The couplings $\Gamma_{L,R}$ are assumed to be constant and

N=0	
$ -5/2, 0\rangle, 5/2, 0\rangle$	$E = 0$
$ -3/2, 0\rangle, 3/2, 0\rangle$	$E = 0$
$ -1/2, 0\rangle, 1/2, 0\rangle$	$E = 0$
N=1, antiferromagnetic (AF)	
$ -5/2, \uparrow_h\rangle, 5/2, \downarrow_h\rangle$	$E = \varepsilon_h - 5/4J$
$ -3/2, \uparrow_h\rangle, 3/2, \downarrow_h\rangle$	$E = \varepsilon_h - 3/4J$
$ -1/2, \uparrow_h\rangle, 1/2, \downarrow_h\rangle$	$E = \varepsilon_h - 1/4J$
N=1, ferromagnetic (FM)	
$ -1/2, \downarrow_h\rangle, 1/2, \uparrow_h\rangle$	$E = \varepsilon_h + 1/4J$
$ -3/2, \downarrow_h\rangle, 3/2, \uparrow_h\rangle$	$E = \varepsilon_h + 3/4J$
$ -5/2, \downarrow_h\rangle, 5/2, \uparrow_h\rangle$	$E = \varepsilon_h + 5/4J$

TABLE I: States for the pure Ising case (Eq. (1) with $J_\perp = 0$). N=0: the six M_z projections of the Mn spin are degenerate. N=1: the presence of a single hole breaks the degeneracy.

f_α^+ ($f_\alpha^- = 1 - f_\alpha^+$) is the Fermi function [11]. In the strong CB regime we only consider states with N=0,1, holes (Table I). The steady state ρ^{stat} , is obtained as $\dot{\rho}(t) = \mathcal{L}\rho^{stat} = 0$, such that \mathcal{L} has a zero eigenvalue with right eigenvector $|0\rangle \equiv \hat{\rho}^{stat}$. The corresponding left eigenvector is $\langle\tilde{0}|\equiv \hat{1}$ such that $\langle\tilde{0}|0\rangle = Tr[\hat{1}\hat{\rho}^{stat}] = 1$ [18], and averages read $\langle\hat{A}\rangle = Tr\{\hat{A}\rho^{stat}\} = \langle\tilde{0}|\hat{A}|0\rangle$.

Shot Noise.— The shot noise spectrum $S(\omega) = 2 \int_{-\infty}^{\infty} d\tau e^{i\omega\tau} \langle\{\Delta\hat{I}(t+\tau), \Delta\hat{I}(t)\}\rangle$ is defined as the Fourier transform of the irreducible (cumulant) correlation function $\langle\{\hat{I}(t+\tau)\hat{I}(t)\}\rangle \equiv \langle\Delta\hat{I}(t+\tau)\Delta\hat{I}(t)\rangle$, where $\Delta\hat{I}(t) = \hat{I}(t) - \langle I \rangle$ measures deviations away from the steady state current $\langle I \rangle$. With the help of the MacDonalds formula [16], $S(\omega)$ can be rewritten as $S(\omega) = \omega \int_0^\infty dt \sin(\omega t) \frac{d}{dt} \langle n^2(t) \rangle$. $\langle n^2 \rangle$ is the variance of the number n of holes being transferred in, say, the right lead in the time interval t . This process is stochastic and is governed by the probability distribution $P_n(t)$ which gives all moments (or cumulants) like, in particular, $\langle n^2 \rangle$. In this context, $P_n(t)$ is expressed in terms of the so-called n -resolved density operator, $\rho^{(n)}(t)$, as $P_n(t) = Tr_{sys}\{\rho^{(n)}(t)\}$ [17]. $\rho^{(n)}(t)$ fulfills a generalized QME $\dot{\rho}^{(n)} = (\mathcal{L} - \mathcal{L}_R^+ - \mathcal{L}_R^-)\rho^{(n)} + \mathcal{L}_R^+\rho^{(n-1)} + \mathcal{L}_R^-\rho^{(n+1)}$. The superoperator \mathcal{L}_R^\pm contains forward/backwards rates. Using the above method, the noise at the right barrier reads:

$$S_{RR}(\omega) = \langle\langle\tilde{0}|\mathcal{J}|0\rangle\rangle - \langle\langle\tilde{0}|\mathcal{I}R(\omega)\mathcal{I}|0\rangle\rangle - (\omega \rightarrow -\omega), \quad (2)$$

$\mathcal{I} \equiv \mathcal{L}_R^+ - \mathcal{L}_R^-$ is the current superoperator (such that $\langle I \rangle = \langle\langle\tilde{0}|\mathcal{I}|0\rangle\rangle$) whereas $\mathcal{J} \equiv \mathcal{L}_R^+ + \mathcal{L}_R^-$ is a superoperator describing self-correlations at the barrier [19]. The pseudoinverse operator is defined as $R(\omega) \equiv Q \frac{1}{i\omega - \mathcal{L}} Q$, where $Q = 1 - |0\rangle\langle\tilde{0}|$ projects out the null space defined by $|0\rangle \equiv \hat{\rho}^{stat}$ [18]. Taking into account the left barrier $S_{LL}(\omega)$ and the noise coming from charge accumulation [20], described by the cross-correlations $S_{LR}(\omega), S_{RL}(\omega)$ [21], the total noise ($\Gamma_L = \Gamma_R$) reads $S(\omega) = \frac{1}{4}\{S_{LL}(\omega) + S_{RR}(\omega) + S_{LR}(\omega) + S_{RL}(\omega)\}$.

Results for $J_\perp = 0$.— The shot noise properties in the $J_\perp = 0$ case are investigated in Fig. 2. The top

panels show results for the $\omega = 0$ shot noise (Fig. 2a) and Fano factor $F = S(0)/2\langle I \rangle$ (Fig. 2b) as a function of V and V_G . At finite bias voltages, $S(0)$ presents steps which depend on V_G . Between plateaus, $S(0)$ changes at values of V where the differential conductance $G_{dc}(V) = d\langle I \rangle/dV$ has maxima (not shown) such that fluctuations are enhanced. In the limit $V \rightarrow 0$, our calculation recovers the fluctuation-dissipation theorem $S(0) = 4kTG_{dc}(0)$, which relates thermal fluctuations (Johnson-Nyquist noise) with the linear conductance. In this linear response regime, both shot noise and linear conductance exhibit a three-peak structure in regions of gate voltage corresponding to charge degeneracy between the $N = 0$ and $N = 1$ sectors (from $V_G = -3$ to $V_G = -5$ in the figure). This is in stark contrast with a normal QD which would exhibit instead one single CB peak. Key for an understanding of this unusual CB is the fact that M_z does not relax during transport [11]: In the absence of holes, the spin of the Mn ion is free and therefore all the six projections M_z are degenerate (Table I, top). Sweeping the gate voltage towards the charge degeneracy region, the only allowed transitions are those which conserve M_z . This results in three possible charge degeneracy points corresponding to the transition $N = 0 \Leftrightarrow N = 1$ at different values of M_z . For example, the first CB peak ($V_G = -3.75$) corresponds to charge degeneracy between $|-5/2, 0\rangle$ and $|-5/2, \uparrow_h\rangle$ (or $|5/2, 0\rangle$ and $|5/2, \downarrow_h\rangle$). The charge degeneracy condition for states with either $M_z = \pm 3/2$ or $M_z = \pm 1/2$ occurs at higher $|V_G|$ (Table I, middle) and, therefore CB is spin-dependent. By further decreasing V_G , we obtain a very small, but finite, three-peak structure which can be attributed to thermal excitations to excited states in the ferromagnetic (FM) sector (Table I, bottom). The above physical picture leads to strong spin-dependent deviations from Poissonian noise (Fano Factor, Fig. 2b). For $|V_G| \leq 5$, the noise remains sub-Poissonian due to spin-dependent CB. For $|V_G| > 5$, the competing dynamics between slow (filled states in the AF sector) and fast channels (FM sector) results in bunching and the noise becomes super-Poissonian [22]. As V increases, FM excited states enter within the bias window and then the noise becomes sub-Poissonian. In this case, bunching of holes at low voltages is replaced by direct hole spin-flips due to tunneling to/from the QD. The results for finite ω are shown in the bottom panels of Fig. 2. At $V_G = -3.75$ (Fig. 2c), shot noise is frequency-independent up to $V \approx 3$. In this voltage region, only states corresponding to the AF sector come into play. Interestingly, at $V \geq 3$ a resonance around $\omega = 0$ develops. The appearance of this resonance can be understood as an enhancement of fluctuations due to tunneling through both AF and FM channels which are now within the bias window. For example, starting from the state $|-1/2, \uparrow_h\rangle$, one hole can tunnel out of the QD leaving the Mn spin in the state $M_z = -1/2$. A second hole can now tunnel

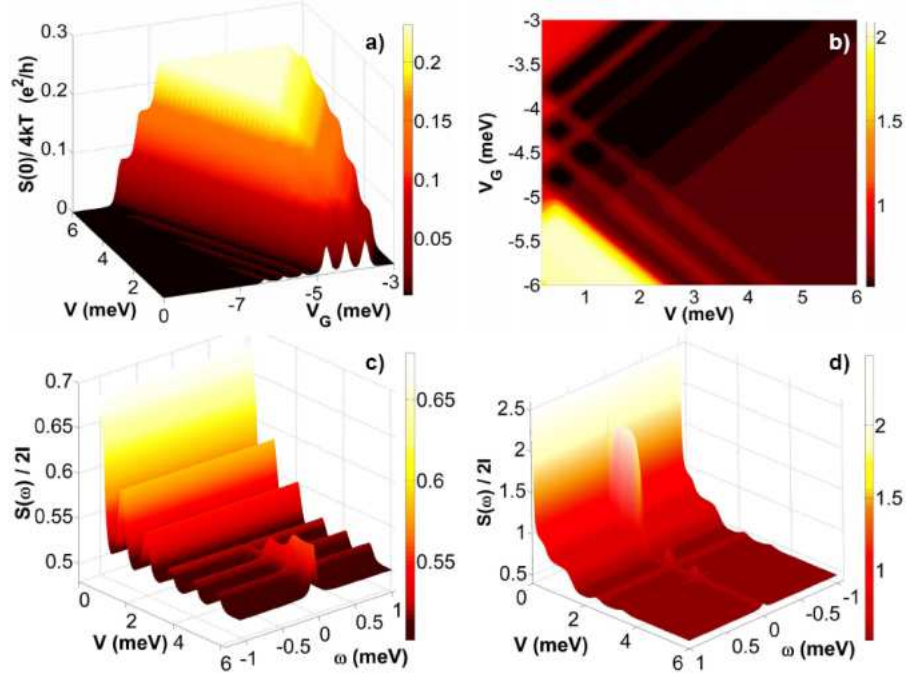


FIG. 2: (Color online) Noise of an artificial SMM for $\alpha = 0$. Top panels: Zero-frequency Shot noise (a) Fano factor (b). Bottom panels: Finite frequency Fano factor, $S(\omega)/2I$ for $V_G = -3.75$ (c) and $V_G = -5.5$ (d). Parameters: $\varepsilon_h = 5$, $J = 1$, $\Gamma_L = \Gamma_R = 0.01$ and $T = 0.05$ (All energies in meV)

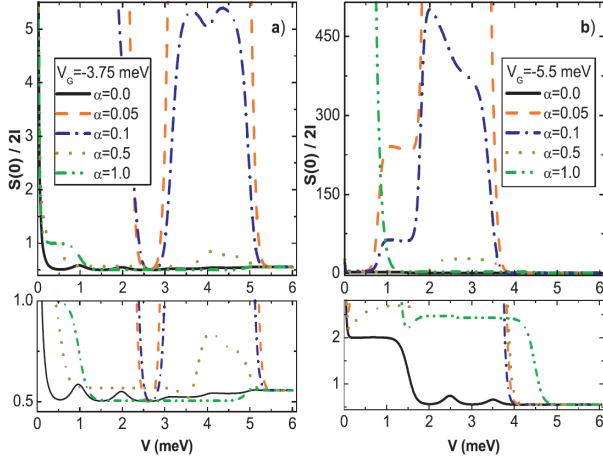


FIG. 3: (Color online) Zero-frequency Fano factors for $\alpha \neq 0$. a) $V_G = -3.75$, b) $V_G = -5.5$ (the rest of parameters are the same as in Fig. 2). Bottom panels: blow up of low Fano factor regions of the corresponding top panels.

onto the state $|-1/2, \downarrow_h\rangle$, which is energetically available, resulting in an effective spin relaxation for the hole (M_z does not change). This mechanism gives rise to a resonance in $S(\omega)$ whose width is given by the inverse hole spin-flip time $1/T_1^h \approx \Gamma$ (other intrinsic hole spin-flip mechanisms, not included here, would also contribute

to this width). Further reduction of V_G allows both kind of channels to participate in transport even at low voltages and the resonance is present for all V (Fig. 2d), in good agreement with our previous interpretation.

Role of spin-flip terms, $J_\perp \neq 0$.— If valence band mixing is nonzero, $|\pm 3/2\rangle$ heavy holes couple with $|\mp 1/2\rangle$ light holes ($J_\perp \neq 0$ in Eq. (1) and $b \neq 0$ in the expressions for $|\uparrow_h\rangle$ and $|\downarrow_h\rangle$). This mixing allows simultaneous spin flips between the hole and the Mn spins [8, 23] which results in split states which are bonding and antibonding combinations of $|M_z = -1/2, \uparrow_h\rangle$ and $|M_z = +1/2, \downarrow_h\rangle$. This splitting can be extracted directly from the $d\langle I \rangle/dV$ curves (not shown here). Fig. 3 illustrates the dramatic changes that mixing induces on noise. As $\alpha = J_\perp/J$ increases, the Fano factor can reach values $F \gg 1$ in voltage regions (both gate and bias) where the noise is sub-Poissonian for $\alpha = 0$ (Fig. 3a). Interestingly, the largest Fano factors are obtained for small values of α : Most of the time, transport events conserve M_z . However, spin-flips mediated by hole transport are small but nonzero. As a result, periods of small current, followed by larger currents, are possible leading to huge Fano factors. We emphasize that super-Poissonian behavior is related here with Mn spin-flips. This is in contrast with the $\alpha = 0$ case where only hole spins can flip. Although we do not seek here a detailed explanation of the various $F \gg 1$ regions for different values of V_G and V , we mention in passing that each particular feature in Figs.

3 can be associated with different transitions between $\alpha \neq 0$ states.

S(ω) and the Dicke effect.— After many transport cycles occur, the Mn spin relaxes completely in some typical time scale $T_1^M \gg T_1^h$: Starting from an empty QD with the Mn in the spin state M_z , a hole tunnels and exchanges one unit of spin with the Mn. After some time $t \approx 1/\Gamma$, the hole tunnels out of the QD such that the Mn spin is now $M_z \pm 1$. Note that it takes many tunneling events to completely relax the Mn spin, such that $T_1^M \gg T_1^h$. This separation of time scales is reflected in $S(\omega)$, which, remarkably, consists of a narrow peak on top of broad resonance (Fig. 4a). The explanation of this feature is a process analogous to the Dicke effect in Quantum Optics [13, 24]: the coupling of both relaxation channels (fast spin hole relaxation and slow Mn spin relaxation) leads to a splitting into two combined decay channels for the whole system. The width of the superradiant channel (broad resonance) allows to extract the hole spin relaxation time as $1/T_1^h$. More importantly, the subradiant channel (narrow resonance) can be used to extract the intrinsic Mn spin-flip time as $1/T_1^M$ in an independent manner. When $\alpha = 0$, only hole spin relaxation is possible (Fig. 4a, solid line). As α changes, a extremely narrow resonance develops on top of the broad one. Furthermore, the difference in magnitude between the noise values at $\omega = 0$ (see previous section) and $1/T_1^h > \omega > 1/T_1^M$ may facilitate the experimental verification of this effect. The broad resonances for $\alpha = 0$ and $\alpha \neq 0$ are very similar, as one expects from our interpretation in terms of hole relaxation. When one of the spin relaxation channels is not available, the Dicke effect should disappear. We have made systematic checks, as a function of V , V_G and α , which corroborate this and demonstrate the robustness of the effect. Fig. 2c, gives a clear demonstration of the absence of Dicke effect when $\alpha = 0$. The opposite case, namely when hole spin relaxation starts to be inefficient, should result in the disappearance of the broad feature in the noise (Fig.4b).

Concluding remarks and experimental consequences.—

In summary, our calculations show that Mn-hole exchange anisotropy has profound consequences on shot noise, like super-Poissonian behavior due to incomplete relaxation of the Mn spin. The main result of this Letter is a novel Dicke effect in the shot noise spectrum that can be used to *separately* measure the spin relaxation times of, both, holes and Mn. Finally, most of the physics captured by our model is inherent to large spin $S > 1/2$ systems with anisotropy. We therefore expect that shot noise measurements in other SMMs, like in the experiments of Refs. [2, 3, 4], may reveal the effects described here. STM spectroscopy of magnetic atoms such as $S = 5/2$ Mn on Cu_2N [25] is one further experimental example where our findings may be relevant.

We thank Joaquín Fernández-Rossier for his input

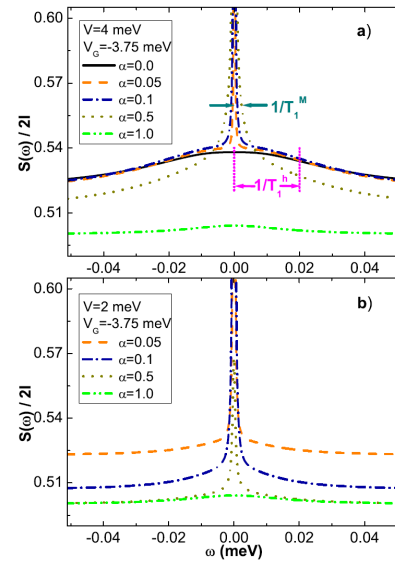


FIG. 4: (Color online) a) Dicke effect in the shot noise spectrum $S(\omega)$ of an artificial SMM. The width of the superradiant channel (broad resonance) allows to extract the spin hole relaxation time as $1/T_1^h$ whereas the subradiant channel (narrow resonance) gives the Mn spin relaxation time as $1/T_1^M$. b) At lower voltages, hole spin relaxation mediated by charge fluctuations is inefficient resulting in a single narrow peak due to Mn spin relaxation. For clarity, we do not show the largest values at $\omega = 0$, see main text.

on the Mn-doped QD model and many useful discussions. Research supported by MEC-Spain (Grant No. MAT2006-03741), CSIC and CAM (Grant No. CCG08-CSIC/MAT- 3775). D. C. acknowledges financial support from Mexican CONACyT ("Consolidación de Grupos de Investigación" Postdoctoral Scholarship).

-
- [1] L. Bogani and W. Wernsdorfer, Nature Materials **7**, 179 (2008).
 - [2] H. B. Heersche, *et al*, Phys. Rev. Lett. **96** 206801, 2006.
 - [3] M.-Ho Jo, *et al*, Nanolett. **6**, 2014 (2006)
 - [4] J. E. Grose, *et al*, Nature Materials **7**, 884 (2008)
 - [5] L. Besombes, *et al*, Phys. Rev. Lett. **93** 207403 (2004).
 - [6] L. Besombes, *et al*, Phys. Rev. B **71** 161307R, (2009).
 - [7] Y. Léger, *et al*, Phys. Rev. Lett. **95** 047403 (2005).
 - [8] Y. Léger, *et al*, Phys. Rev. Lett. **97** 107401 (2006).
 - [9] L. Besombes, *et al*, Phys. Rev. B **78**, 125324 (2008)
 - [10] J. Fernández-Rossier and R. Aguado, Phys. Stat. Sol. (c) **3** 3734 (2006).
 - [11] J. Fernández-Rossier and R. Aguado, Phys. Rev. Lett. **98** 106805 (2007).
 - [12] Ya. M. Blanter and M. Büttiker, Phys. Rep. **336** 1 (2000).
 - [13] R. H. Dicke, Phys. Rev. **93**, 99 (1953).
 - [14] Strain-induced anisotropy terms of the form $D(M^z)^2$ are very small as compared to Mn-hole exchange. This anisotropy is, however, important when the Korringa

- mechanism contributes to Mn spin relaxation in the absence of carriers. See Ref. [9].
- [15] When $\alpha = 1$, we recover the physics of an isotropic Heisenberg model, which can be used to model electron transport as well. This kind of model has been used extensively in the literature to model SMMs coupled to electrodes. See, e.g., F. Elste and C. Timm, Phys. Rev. B **71**, 155403 (2005); C. Romeike *et al* Phys. Rev. Lett. **97**, 206601 (2006); K.-I. Imura *et al* Phys. Rev. B **75**, 205341 (2007); G. Kiesslich *et al*, arXiv:0906.1986.
 - [16] D. K. C. MacDonald, Rep. Prog. Phys. **12**, 56 (1949).
 - [17] Similarly to photon counting in Quantum Optics, $\hat{\rho}(t)$ is unravelled with respect to n , $\hat{\rho}(t) = \sum_n \hat{\rho}^{(n)}(t)$. See, e. g., M. B. Plenio and P. L. Knight, Rev. Mod. Phys. **70** (1998) 101.
 - [18] This projection guarantees that the $\omega \rightarrow 0$ limit is well defined, namely $R(\omega \rightarrow 0) = Q\mathcal{L}^{-1}Q$ inverts the Liouvillian in a subspace spanned by the operator Q such that the inverse of the Liouvillian is not ill-defined. See, e.g., C. Flindt, T. Novotný and A. -P. Jauho, Phys. Rev. B **70** (2004) 205334.
 - [19] The Markov approximation neglects the frequency-dependence of the jump operators. As a result, quantum noise effects at $\hbar\omega > V$ are not taken into account (D. Marcos *et al*, in preparation, 2009).
 - [20] R. Aguado and T. Brandes, Phys. Rev. Lett. **92** 206601 (2004).
 - [21] N. Lambert, R. Aguado and T. Brandes, Phys. Rev. B **75**, 045340 (2007).
 - [22] W. Belzig, Phys. Rev. B **71** (2005) 161301(R).
 - [23] J. Fernández-Rossier, Phys. Rev. B **73**, 045301 (2006).
 - [24] Dicke superradiance of photons in molecular nanomagnets has been discussed in E. M. Chudnovsky and D. A. Garanin, Phys. Rev. Lett. **89**, 157201 (2002). Here, the role of photon emission is played by hole transport.
 - [25] C. Hirjibehedin *et al*, Science **317**, 1199 (2007).